Ab initio study of the pseudorotation and conformational stability of pyrrolidine

Luis Carballeira * and Ignacio Pérez-Juste

Departamento de Química Física, Universidad de Vigo, Apdo. 874, 36200 Vigo, Spain

The energy profile for the pseudorotational process of pyrrolidine has been investigated with several *ab initio* computational methods, and both stable conformers and transition states have been characterized. Theoretical calculations show that pseudorotation is the path preferred for interconversion between the N–H axial and equatorial forms, with a barrier of approximately 0.6 kcal mol^{-1}. MP2/6-31G results agree acceptably well with the experimental data from microwave spectroscopy, electron diffraction and vibrational frequencies, which suggest that electron correlation is needed to obtain a reliable description of the conformational preferences. The existence of a free-pseudorotation region predicted by correlated calculations allows the contradictions between the previously reported interpretations of experimental work to be eliminated. The natural bond orbitals (NBO) method was applied on the HF/6-31G** wavefunctions to confirm the existence of delocalization due to the nitrogen lone pair. The relationship between delocalization and the puckering of the axial and equatorial envelope forms is discussed.**

Introduction

The conformational analysis of saturated five-membered rings has long been the subject of experimental[1–7] and theoretical studies.[7–10] These rings can invert their conformation passing through different envelope and twist forms, in a movement that has certain characteristics of rotation, but without contributing to the angular moment because the atoms move perpendicularly to the ring. For this reason it is named pseudorotation, a concept first put forward by Kilpatrick *et al.*[11] to explain the high value of the entropy of cyclopentane. According to Pople and Cremer,[12–14] two coordinates suffice to describe pseudorotation: the puckering amplitude q, which represents the deviation of the ring from planarity, and the pseudorotational phase angle φ, which indicates the position of the ring in the pseudorotational path. Among the saturated five-membered rings, pyrrolidine (PYR) is especially interesting due to its presence in numerous compounds of biological interest, such as amino acids and peptides. The N–H axial and equatorial envelope conformations of PYR, which correspond to the forms E1 ($\varphi = 0°$) and E6 ($\varphi = 180°$) shown in Fig. 1, can be interconverted by pseudorotation passing through ten envelope forms (E1–E10) situated at intervals of $\varphi = 36°$ (= 360°/10), between which the same number of twist forms are inserted (T1–T10), not shown in order to simplify the figure.[13] Pseudorotational barriers for cyclopentane (CPT) or tetrahydrofuran (THF) are practically negligible, ~0[4,8] and ~0.2–0.4[5–7] kcal mol^{-1}, respectively. However, there is a certain scattering in the published data for PYR, both in the height of the pseudorotational barrier and in the characterization of the stable conformers. Hence, thermodynamic studies[15–17] show that the pseudorotation of PYR is free or practically free, while McCullough *et al.*[17] obtain a barrier of 300 cal mol^{-1}, and Pitzer and Donath,[18] as a result of calculations based on strain energies, give a value of 1.3 kcal mol^{-1} and predict that the twist conformer T1 is the most stable. Other experimental studies fail to clarify both the height of the barrier and the conformational preferences.[19–25] Oberhammer *et al.*[26] compared the rotational constants and the imino hydrogen r_s coordinates obtained by microwave spectroscopy, with the constants estimated for different conformations of PYR throughout the process of pseudorotation. A reasonable correlation was found between the experimental and calculated results for the forms E1 and T1 (originally[26] termed B1-ax and T3-ax), even though the authors disregard T1, because the agreement in the hydrogen coordinates is produced at the expense of the inversion of the rotational constants. In the microwave spectrum, the equatorial conformer is not present because all the intense lines can be assigned to the axial conformer, and it is not possible to estimate the difference in energy between the two forms. Subsequently the same authors,[27] through a combined study using electron diffraction and *ab initio* HF/4-21G(N*) calculations, predict that the axial conformer E1 is more stable than the equatorial conformer E6 by 0.97 kcal mol^{-1}, and determine a height of around 1.66 kcal mol^{-1} for the pseudorotational barrier. More recently, and during the elaboration of this work, Kang *et al.*[28] applied a revised pseudorotational model for the puckering of heterocyclic five-membered rings to their HF/6-31G** and MP2/6-31G** results for PYR. By means of restrained geometrical optimizations and without further characterization of the optimized conformations, a pseudorotational barrier of 0.8 kcal mol^{-1} was estimated, and the MP2 results on structures and energetics were found to be consistent with diffraction and spectroscopic experiments.

In previous papers,[29,30] we analysed the influence of the computational level on the N–H axial–equatorial equilibrium of saturated six-membered rings containing nitrogen and the effect of the nitrogen lone pair delocalization both on the geometry and energy of these rings. However, to our knowledge, a similar theoretical study of an analogous compound such as PYR has not been carried out. Therefore, we present in this work the characterization of the stationary points on the potential energy surface of PYR and an in depth analysis of the influence of the basis set and electron correlation on the pseudorotational barrier and conformational preferences, employing HF SCF,[31–34] and MP2, MP3 and MP4 computational methods.[35–38] The natural bond orbitals (NBO) method[39–43] was used to establish the factors which determine the conformational stabilities, and the geometrical effects associated with the delocalization of the nitrogen lone pair were examined. Finally, we compare the theoretical results obtained with the experimental data available.

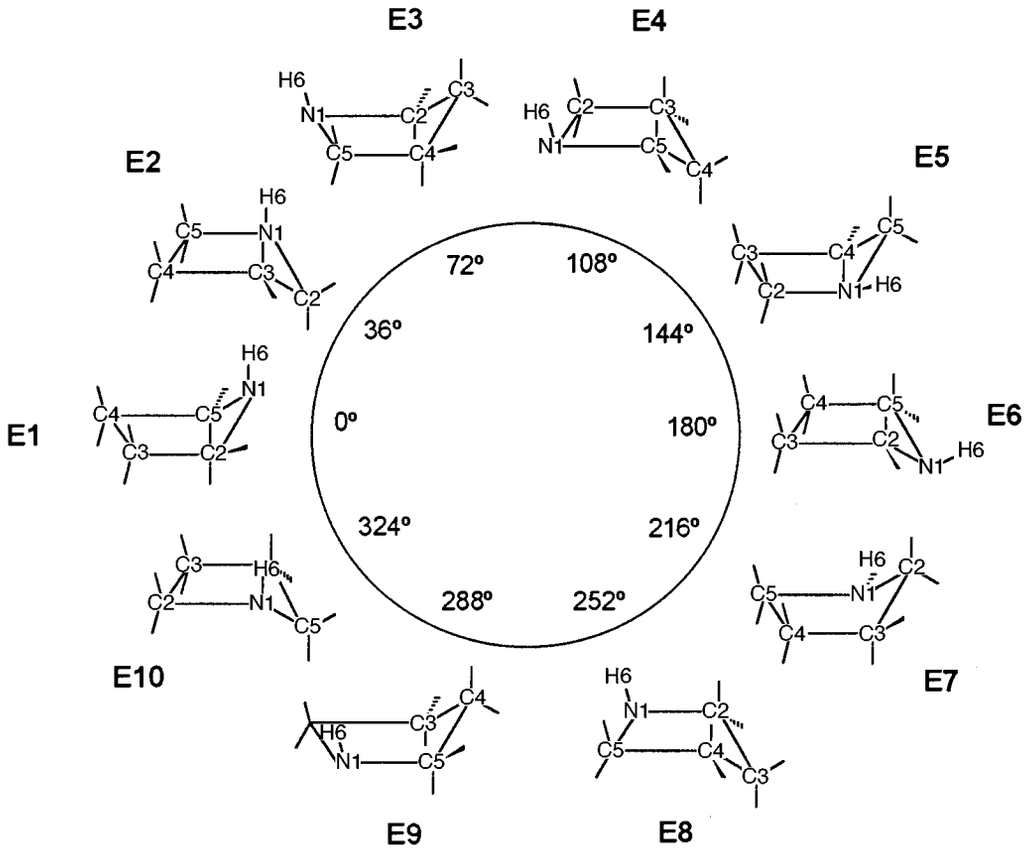

Fig. 1 Envelope conformations of pyrrolidine along the pseudorotational path. The twist conformations are located between adjacent envelope forms. See Fig. 3 for complete numbering.

Methods

In order to study the pseudorotational barrier of PYR, the envelope conformations from E1 to E6 shown in Fig. 1 have been optimized using the HF/3-21G, HF/6-31G** and MP2/6-31G** computational levels, restraining to zero the torsional angle corresponding to the atoms which are found in the plane of each conformation.[27] Calculations on these forms suffice because, by symmetry, the pairs E2/E10, E3/E9, E4/E8 and E5/E7 correspond to the same conformation. Single-point calculations have been carried out on the HF/6-31G** and MP2/6-31G** optimized geometries using the 6-311G**, 6-31++G** and 6-311++G** basis sets. On the MP2/6-31G** geometries, MP3 and MP4(SDTQ) single-point calculations have also been performed using the 6-31G** basis set. Once the profile of the pseudorotational energy curve had been determined, the conformations situated around the regions of minimum and maximum energy were optimized without restrictions and characterized as minima or transition states by means of the analysis of their vibrational frequencies at the HF/3-21G, HF/6-31G** and MP2/6-31G** levels. The correction of zero point energy (ZPE) was also evaluated. To determine which process of interconversion is energetically preferable, the planar form of PYR has also been studied employing the same methods indicated above.

Due to the presence of the nitrogen lone pair, some effects associated with the delocalization of the pair may be possible. For this reason the NBO analysis[39–43] has been carried out on the HF/6-31G** wavefunctions, since this method has been successfully used in six-membered rings containing nitrogen where delocalization effects are present.[29,30,44,45] The NBO method transforms the Hartree–Fock molecular orbitals into a set of localized orbitals which form a hypothetical Lewis structure with strictly localized electron pairs. The energy of this structure (E_{Lew}) includes steric and electrostatic effects which cannot be separated by means of the NBO method. The difference between E_{Lew} and the total SCF energy (E_{rel}), evaluated using the NBO deletion procedure, corresponds to the energetic contributions of all the interactions between occupied orbitals and antibonds, that is, the delocalization energy, E_{del}. Orbital interactions such as n_N–σ^*_{C-H} and n_N–σ^*_{C-C} are dominant, but smaller interactions between adjacent bonds and antibonds may also make different relative contributions to the E_{del} of each conformer. Both the *ab initio* calculations and the NBO analysis were carried out using the Gaussian 94 program.[46]

Results and discussion

Pseudorotational barrier and conformational preferences: influence of the computational level

The pseudorotational energy curves obtained at various computational levels are shown in Fig. 2 and the relative energies of the stationary points found are listed in Table 1. With all the computational levels employed, we have also performed the unrestricted geometrical optimization of an initial planar structure of PYR, and a quasi-planar conformation (PL) was always obtained corresponding to a transition state with two imaginary vibrational frequencies. In agreement with the MP2 calculations of Kang *et al.*,[28] this PL form was found to be clearly more energetic (>5 kcal mol^{-1}) than the envelope and twist forms located along the pseudorotational path. It should be noted, however, that our MP2 geometries for the PL form (see Table 2) differ from those of reference 28, where a completely planar structure was reported, probably because in that work only restricted geometrical optimizations were performed. In any case, according to previous work, the preferred process for interconversion between the different conformations of PYR is pseudorotation and not inversion through the planar form.

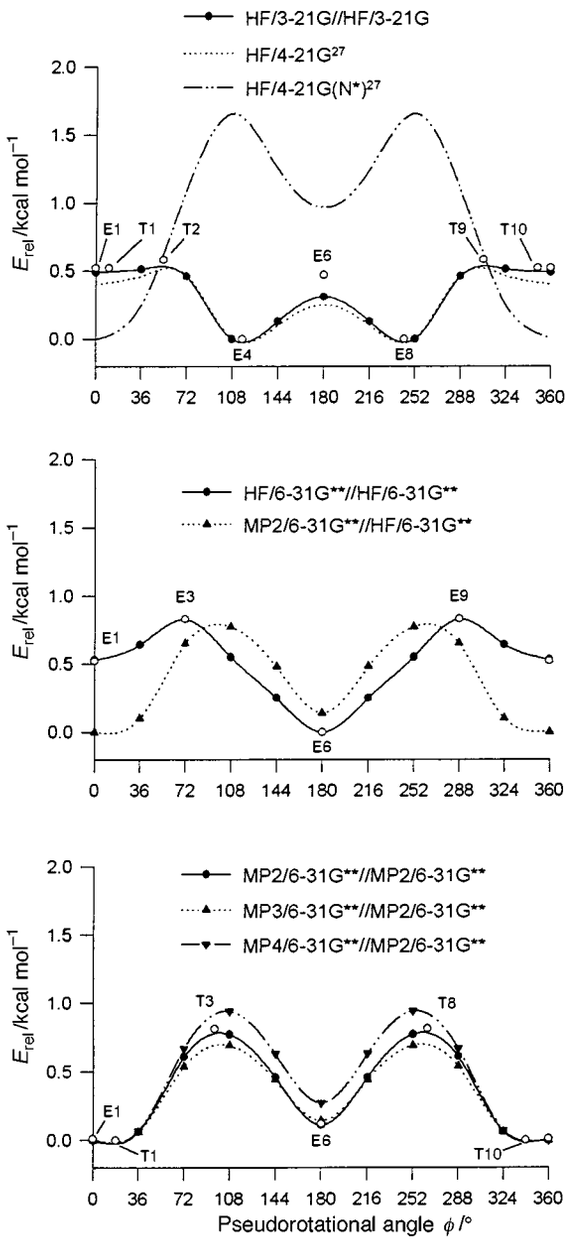

Fig. 2 Pseudorotational energy profiles of pyrrolidine calculated at several computational levels. Stationary points at each level are also represented as open circles. See text and Table 1.

With regard to the pseudorotational energy profiles, the most striking feature is the notable discrepancy between the HF/3-21G curve and the others. At this level, the approximate conformations T1/T10 ($\varphi = 10.5$, 349.5°) and E4/E8 ($\varphi = 108$, 252°) have been characterized as minima, and E1 ($\varphi = 0°$) and E6 ($\varphi = 180°$) as transition states. However, according to the HF/6-31G** results, the N–H axial (E1) and equatorial (E6) envelope forms are the stable conformers. Oberhammer found a similar discrepancy when using HF/4-21G and HF/4-21G(N*) calculations (included in Fig. 2).[27] It can be seen that the energy profiles obtained with non-polarized basis sets (3-21G and 4-21G) are similar, whereas the 4-21G(N*) and 6-31G** curves are remarkably different and the stabilities of the minima are inverted. The pseudorotational curves calculated using larger basis sets such as 6-311G**, 6-31++G** and 6-311++G** (not represented in Fig. 2 in order to simplify the diagram) are similar to the HF/6-31G** one, in spite of minor numerical differences. As can be seen in Table 1, when augmenting the size of the basis set, the energy differences E1–E6 increase from 0.52 to 0.67 kcal mol^{-1}, and the height of the pseudorotational barrier oscillates slightly around 0.8 kcal mol^{-1}. To summarize, the discrepancy between the different HF results suggests that non-polarized (3-21G or 4-21G) or unbalanced [4-21G(N*)] basis sets are unsuitable for the description of the pseudorotation of PYR. On the other hand, polarized basis sets like 6-31G** and larger ones, predict similar energy curves, even though the energy differences E1–E6 seem not to converge, at least not with the group of basis sets used in this work.

As shown in Fig. 2, the effect of electron correlation in the description of the pseudorotational potential is important, since the curves obtained using correlated calculations differ markedly from the HF/6-31G** one. Two aspects should be remarked upon: (a) MP2/6-31G**//MP2/6-31G** and MP2/6-31G**//HF/6-31G** calculations predict similar pseudorotational curves, which suggests that the effect of electron correlation does not depend on the geometry employed; (b) the MP3 and MP4 curves do not differ substantially from the MP2 ones already mentioned, which indicates that perturbative correlated levels higher than MP2 do not significantly improve the results. The HF/6-31G** stabilities are inverted at any of the MP levels. The equatorial minimum E6 is less stable than E1, and the energy differences E6–E1 are smaller than the HF values (0.12, 0.14 and 0.28 kcal mol^{-1}, for MP2, MP3 and MP4, respectively). Although the HF/6-31G** and MP curves also differ in the position of the energy maximum, the pseudorotational barriers are quite similar (0.83 *vs.* 0.77, 0.69 and 0.94 kcal mol^{-1}), which confirms that pseudorotation in PYR is more restricted than in CPT or THF. The effect of ZPE is similar at HF/6-31G** and MP2/6-31G** levels and contributes to the reduction of height of the barrier by approximately 0.2 kcal mol^{-1}, while not affecting the energy difference between minima. The region of the MP curves near 0° deserves special attention, since the energy profile suggests that the energy minimum does not correspond exactly with an E1 form ($\varphi = 0°$). Indeed, the MP2/6-31G** vibrational analysis for E1 shows an imaginary frequency (31i cm^{-1}), corresponding to a normal mode of pseudorotation, which indicates that we are dealing with a transition state. Some conformations around E1 have been freely optimized, and an energy minimum (with zero imaginary frequencies) has been localized with a pseudorotational angle $\varphi = 18°$, which corresponds to the twist form T1/T10 (see Fig. 3). The energy differences between E1 and T1 are practically negligible at all MP levels, which suggests that the pseudorotational motion in an approximate interval between $\varphi = 324°$ and $\varphi = 36°$ is free.

The influence of the basis set at the MP2 level does not follow a clear trend as in HF. Again, the curve profiles (not reported in Fig. 2) are similar with all the basis sets, but the E6–E1 difference invert even when using 6-31++G** and 6-311++G**, so E6 turns out to be more stable. On the contrary, the height of the barrier is not very sensitive to the basis set. Although, it has been suggested that the MP2 energy corrections may be artifacts depending on the size of the basis set,[44,45] relative energies do not allow us to establish with certainty the influence of the basis set on the relative stabilities at the MP2 level. Unfortunately, due to computational limitations, it was not possible to carry out MP2, MP3 or MP4 calculations with basis sets larger than those used in each case, therefore the effect of the size of the basis set should be the subject of further study in the future.

Geometrical features: delocalization and ring puckering

Table 2 displays the optimized geometries and puckering coordinates of the MP2/6-31G** stationary points of PYR,[47] which are represented in Fig. 3. The results obtained for CPT were also included, since the comparison with PYR provides us with information about the effect of nitrogen on a ring of only carbon atoms. As expected, the envelope (E, C_s symmetry) and twist (T, C_2 symmetry) forms of CPT have the same energy at all the computational levels, indicating free pseudorotation.[3,4] With regard to the geometries, it is known that, at the HF level,

Table 1 Relative stabilities and zero-point energies (in kcal mol^{-1}) for the stationary points of pyrrolidine at several computational levels. The values in brackets in the ZPE column are the lowest vibrational frequencies (in cm^{-1}, not scaled). See text for further calculations details

HF/3-21G geometries

	3-21G	ZPE
E1	0.52	86.97 (12i)
T1	0.52	86.99 (16)
T2	0.58	86.87 (53i)
E4	0.00	86.86 (78)
E6	0.47	86.98 (48i)
PL	4.26	86.47 (207i, 201i)

HF/6-31G** geometries

	6-31G**	ZPE	6-311G**	6-31++G**	6-311++G**	MP2/6-31G**
E1	0.52	87.03 (33)	0.61	0.66	0.67	0.00
E3	0.83	87.83 (70i)	0.73	0.85	0.79	0.64
E6	0.00	87.05 (62)	0.00	0.00	0.00	0.14
PL	4.83	86.71 (232i, 208i)				

MP2/6-31G** geometries

	6-31G**	ZPE	6-311G**	6-31++G**	6-311++G**	MP3/6-31G**	MP4/6-31G**
E1	0.01	83.72 (31i)	0.07	0.48	0.18	0.00	0.00
T1	0.00	83.78 (41)	0.00	0.43	0.13	0.00	0.00
T3	0.81	83.55 (70i)	0.94	0.74	0.64	0.72	0.95
E6	0.12	83.74 (65)	0.30	0.00	0.00	0.14	0.28
PL	6.12	83.54 (252i, 224i)					

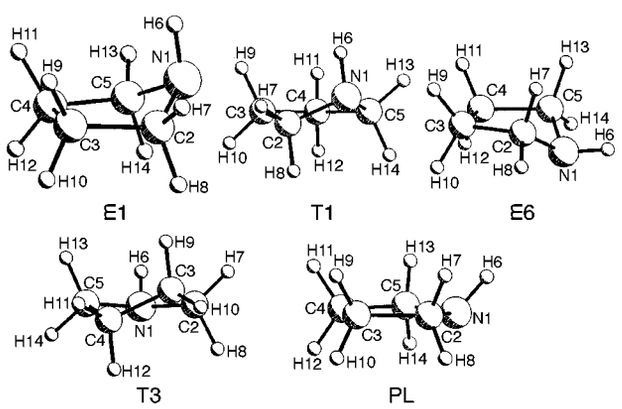

Fig. 3 MP2/6-31G**//MP2/6-31G** optimized structures for the stationary points of pyrrolidine

the increase in the size of the basis set and particularly the introduction of polarization increases the electronic density in the bonding region.[48,49] Thus, when passing from HF/3-21G to HF/6-31G** geometries in CPT, C–C bonds become shorter and the repulsion between adjacent bonds increase, hence the bond angles widen and the endocyclic torsions are reduced. As a consequence of these geometric modifications, the ring is flattened as indicated by the values of the puckering amplitude q (0.415 and 0.402 Å). When MP2 electron correlation is introduced, the electronic density is redistributed, increasing around the nuclei and diffuse regions of the molecule, whereas it decreases in the bonding region, hence steric repulsions are reduced.[48,50] Thus, MP2/6-31G** C–C bonds are shorter than HF/6-31G**, C–C–C bond angles close and the torsions widen slightly, hence the MP2 optimized ring puckers compared with the HF one, and there is an increase in the coordinate q (0.420 Å). In summary, at the HF level, the 6-31G** ring is flatter than the 3-21G one, due principally to the increase in steric repulsions, which are reduced when including electron correlation, whereby the ring puckers again. As the variation of the puckering amplitude with the calculation level is the same for PYR and CPT, q(6-31G**) < q(3-21G) < q(MP2), it seems to be associated with the computational method used independent of the system which is the object of study.

It is also interesting to compare the variation of the puckering amplitude throughout the process of pseudorotation. For CPT, the value of q for the E and T forms are the same, and do not vary during the course of pseudorotation, which indicate that the inversion of the ring by pseudorotation follows a circular path with a radius q, in the system of coordinates (q, φ).[13] The same effect was observed for THF by Cadioli *et al.* employing MP2/6-31G*(5D) calculations.[7] However, for PYR, as shown in Fig. 4, the behaviour of q is noticeably different, since the puckering amplitude increases between $\varphi = 0 \rightarrow 180°$, and decreases to $\varphi = 360°$ due to symmetry. This means that the pseudorotational path of PYR is not circular but elliptical, because the radius q changes throughout the process. The values of q indicate that the N–H axial form E1 is always flatter than E6. At the same time, with all the computational levels used, E1 is less puckered than the E conformer of CPT. However, E6 is more puckered than CPT using MP2/6-31G** calculations, whereas HF/3-21G and HF/6-31G** levels predict almost the same puckering amplitudes. According to the optimized geometries, the main factor responsible for this behaviour of q is the modification of the N1–C2–C3 angle and the associated N1–C2–C3–C4 torsion compared to the corresponding parameters of CPT. It can be observed (Table 2) that N1–C2–C3 opens in E1 and closes in E6, whereas N1–C2–C3–C4 is modified in the opposite way. The variations of the latter torsional angle are parallel to the variations of q. Thus, the N1–C2–C3–C4 torsion in E1 closes between 2 and 3° with respect to C1–C2–C3–C4 in CPT, and q also decreases, while the puckering amplitude for E6 increases as a consequence of the widening of the N1–C2–C3–C4 torsional angle.

In addition to the N1–C2–C3 angles and the N1–C2–C3–C4 torsions, other coordinates (H8–C2, C2–C3, H8–C2–N1, H8–C2–N1–C5) also present variations, in both directions, with regard to the corresponding values in the envelope form of CPT (Table 2). The behaviour of these geometric parameters is related to the delocalization of the nitrogen lone pair. It has been established that the bonds in a *trans* orientation to a lone pair become longer and the associated angles open, compared

Table 2 Selected MP2/6-31G** geometrical parameters (Å and °) for the stationary points of cyclopentane (CPT, X1 = C1) and pyrrolidine (PYR, X1 = N1).[47] Pople and Cremer's puckering coordinates (q in Å, φ in °)

	CPT		PYR					
	E	T	E1	T1	T3	E6	PL	Exp[27]
X1–C2	1.5285	1.5473	1.4686	1.4676	1.4797	1.4634	1.4706	1.469(10)
C2–C3	1.5392	1.5322	1.5439	1.5365	1.5294	1.5340	1.5415	1.543(8)
C3–C4	1.5512	1.5275	1.5465	1.5435	1.5265	1.5480	1.5401	1.543(8)
C4–C5	1.5392	1.5322	1.5439	1.5519	1.5278	1.5340	1.5415	1.543(8)
C5–X1	1.5285	1.5473	1.4686	1.4711	1.4771	1.4634	1.4706	1.469(10)
H6–X1	1.0933	1.0901	1.0181	1.0179	1.0115	1.0154	1.0101	1.020
H7–C2	1.0901	1.0899	1.0894	1.0895	1.0911	1.0900	1.0934	1.090(4)
H8–C2	1.0926	1.0917	1.0924	1.0929	1.0936	1.1006	1.0924	1.090(4)
X1–C2–C3	103.88	104.99	106.96	106.06	105.90	102.31	107.66	104.6
C2–C3–C4	105.67	102.82	104.01	103.47	101.62	104.20	106.69	104.9
C3–C4–C5	105.67	102.82	104.01	104.16	102.13	104.20	106.69	104.9
C4–C5–X1	103.88	104.99	106.96	107.70	104.43	102.31	107.66	104.6
C5–X1–C2	102.40	105.86	102.72	103.04	108.42	103.66	111.11	105.2(32)
H6–X1–C2	109.87	111.31	107.56	107.25	110.12	111.45	110.15	107.0
H7–C2–X1	113.61	112.69	110.73	110.82	111.27	110.98	111.09	
H8–C2–X1	109.02	109.96	107.59	107.82	109.46	112.63	109.99	
X1–C2–C3–C4	25.44	35.09	23.39	32.26	30.99	27.72	2.58	
C2–C3–C4–C5	0.00	−43.47	0.00	−11.40	−41.15	0.00	0.00	
C3–C4–C5–X1	−25.44	35.09	−23.39	−12.77	36.80	−27.72	−2.58	
C4–C5–X1–C2	41.31	−13.37	38.09	32.81	−17.72	46.85	−4.38	
C5–X1–C2–C3	−41.31	−13.37	−38.09	−40.47	−8.45	−46.85	4.38	
H6–X1–C2–C3	75.40	107.17	75.23	72.99	111.98	−166.83	126.72	
H8–C2–X1–C5	76.01	103.88	80.15	77.59	110.00	70.81	124.91	
H7–C2–X1–C5	−164.23	−136.72	−162.36	−164.50	−131.63	−167.90	−117.10	
φ	0.00	90.00	0.00	17.99	96.36	180.00	0.00	
q	0.421	0.421	0.369	0.373	0.410	0.452	0.041	0.38(2)

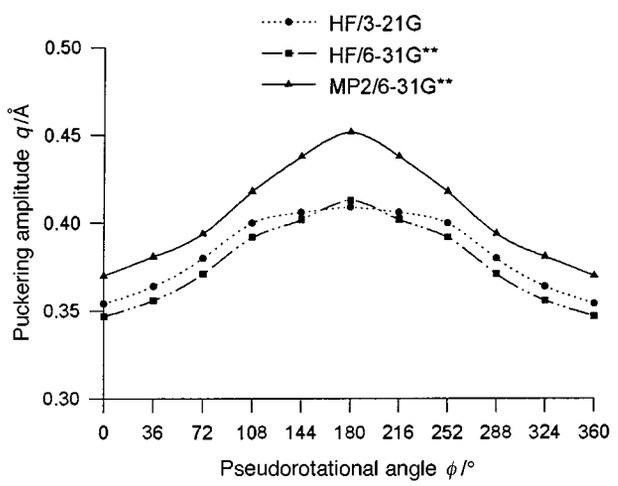

Fig. 4 Variation of the puckering amplitude q during the pseudorotation of pyrrolidine calculated with several computational models

with those not *trans* oriented.[51] Thus, the C2–C3 bond is longer in the axial E1 form, and H8–C2 is lengthened in E6, due to their *trans* orientation to the lone pair. Similar variations can be observed in the N1–C2–C3 and H8–C2–N1 angles, which open when the bonds are lengthened. Therefore, it can be concluded that the puckering of the axial and equatorial forms of PYR is determined by the geometrical effects associated with the delocalization of the nitrogen lone pair. It also should be noted that, although absolute values of bond lengths or bond angles depend on the theoretical level used, the trends associated with the delocalization of the lone pair are similar for all the geometries calculated.[47]

The confirmation of the existence of geometrical trends associated with the delocalization of the nitrogen lone pair has led us to use the NBO analysis on the HF/6-31G** wavefunctions. According to the NBO energy contributions

Table 3 HF/6-31G** relative energies (E_{rel}), Lewis energies (E_{Lew}), and hyperconjugation contributions (E_{del}) for the N–H axial E1 and equatorial E6 forms of pyrrolidine (in kcal mol^{-1}). Dipole moments (μ/D) are also shown

	E_{rel}	E_{Lew}	E_{del}	μ
E1	0.52	−2.35	2.87	1.43
E6	0.00	0.00	0.00	1.05

obtained for the stable conformers (Table 3), E6 is more stable because the hyperconjugative stabilization (delocalization) is greater than the destabilization indicated by E_{Lew}. The analysis of the second-order matrix indicates that n_N–σ^*_{C-H} interactions in E6 are stronger, and therefore more stabilizing than n_N–σ^*_{C-C} in E1. With regard to the Lewis energies, dipolar interactions do not seem to be determinant in the stabilization of E1, since the dipole moments of E1 and E6 are similar. Hence, the main factor responsible for the Lewis term could be the presence of steric interactions between the substituent of the nitrogen in the apex of the ring (N–H or N–Lp) and the opposed C–H groups. As was indicated previously, E1 is flatter than E6, so the substituent on the nitrogen and the opposed C3–H and C4–H groups are more separated, which would cause the steric interactions in E1 to be smaller. The lengthening of the bonds C2–C3 and C4–C5 in E1 as a consequence of the delocalization of the nitrogen lone pair would also contribute to the separation of these groups. Unfortunately, our computational limitations prevent us from carrying out the NBO analysis on the correlated wavefunctions, hence, due to the differences between the conformational stabilities obtained at HF and MP levels, the HF/6-31G** NBO analysis should be taken into account with caution.

Comparison between experiment and theory

The experimental geometries obtained by electron diffraction, also included in Table 2, were assigned by Oberhammer *et al.*[27] to the E1 conformer, using certain restrictions based on their

Table 4 Theoretical and experimental[26] rotational constants and imino hydrogen (H6) coordinates for some conformations of pyrrolidine

	Rotational constants (MHz)				H6 coordinates (Å)		
	A	*B*	*C*	κ[a]	|*a*|	|*b*|	|*c*|
Microwave	6834.54	6677.84	3888.06	0.8936	1.3439	0.1505	1.2122
MP2/6-31G**							
E1	6903.15	6711.34	3922.34	0.8713	1.2722	0.0000	1.2350
T1	6906.48	6713.20	3926.20	0.8703	1.2937	0.0625	1.2204
E6	6925.60	6849.50	3945.17	0.9489	2.1205	0.0000	0.0314

[a] Asymmetry parameter $\kappa = (2B - A - C)/(A - C)$

Table 5 Selected experimental[20] and theoretical vibrational frequencies (in cm^{-1}) for some conformations of pyrrolidine

	HF/6-31G**[a]		MP2/6-31G**[b]			Exp.	
	E1	E6	E1	T1	E6		
ν(N–H)	3337	3372	3379	3382	3418	3320	3362
ν_{asym}(C–H)	2890	2881	3041	3041	3024	2962	2930
ν_{sym}(C–H)	2843	2768	2976	2979	2888	2872	2821

[a] Scaled by a factor of 0.89. [b] Scaled by a factor of 0.95.

HF/4-21G(N*) calculations, that is, equal C–C and C–H bond lengths, equal H–C–H angles, local C_{2v} symmetry for the CH_2 groups and a fixed position for the hydrogen bonded to the nitrogen. In accordance with the conclusions of Kang *et al.*,[28] the best numerical agreement between these experimental data and the theoretical results corresponds to the MP2/6-31G** geometries.[47] However, it should be pointed out that the geometries for both E1 and T1 are compatible with the experimental results. Thus, the puckering amplitudes and the average values for the N–C, C–C and C–H bond lengths of both forms (E1: $r_{NC} = 1.469$, $r_{CC} = 1.545$, $r_{CH} = 1.091$ Å; T1: $r_{NC} = 1.469$, $r_{CC} = 1.544$, $r_{CH} = 1.091$ Å) notably agree with the experimental values. Therefore, MP calculations suggest that, as a consequence of the free pseudorotation in the vicinity of $\varphi = 0°$, the electron diffraction data should be produced by an average of the geometries of the conformations interchanging freely during pseudorotation.

On the other hand, Table 4 shows the rotational constants and the r_s coordinates of H6 obtained by microwave spectroscopy, which have also been interpreted as being compatible only with the axial form E1.[26] If a comparison is made between the experimental data and the MP2/6-31G** results, it can be seen that there are appreciable discrepancies between the experimental and calculated values for the equatorial form E6. However, the agreement for E1 and T1 is similar, and, in contrast to reference 26, no inversion is observed in the r_s coordinates of H6 in T1, hence neither of these two forms can be discarded. This observation, together with what was previously stated with regard to the electron diffraction data, suggests that the conclusion that PYR adopts only an N–H axial envelope conformation[26,27] is perhaps too definitive, since, according to our theoretical predictions of free pseudorotation in the interval 324°–36°, there should exist similar proportions of the E1 and T1 forms, which would contribute to the electron diffraction and microwave spectra. The coexistence of both forms would also explain the experimental deviation of |*b*| (0.1505 Å) with regard to the expected value of 0 Å corresponding to the E1 conformer because of its C_s symmetry (Table 4).

Finally, amongst the effects associated with the delocalization of the nitrogen lone pair, the following are known:[52] the increase of the ν(N–H) frequencies, and the reduction of the ν(C–H) frequencies for C–H bonds *trans* oriented to the lone pair, which are known as Bohlmann bands.[53] These trends can be observed in the experimental frequencies for the N–H bond and the axial C–H bonds adjacent to the nitrogen (Table 5). These results were interpreted by Krueger and Jan[20] in terms of a mixture of two conformations, which correspond to E8 and E3 in Fig. 1, where the nitrogen lone pair is *trans* oriented or not to an adjacent C_2–H bond. From the temperature dependence of the N–H bands, it was estimated[20] that the *trans* lone pair/C–H orientation is ~0.2 kcal mol^{-1} more favourable. Kang *et al.*[28] indicated that this experimental value is similar to the MP2/6-31G** energy difference (0.1 kcal mol^{-1}) between the N–H axial and equatorial envelope conformers (E1 and E6, respectively). However, the numerical agreement between both interpretations could be fortuitous because the E8 and E3 forms of reference 20 are not energy minima and Kang *et al.* had not considered different forms from E1 and E6 to compare both experimental and theoretical values. As can be seen in Table 5, the HF/6-31G** and MP2/6-31G** vibrational frequencies for the stable envelope conformers reproduce the experimental tendencies associated with the delocalization of the nitrogen lone pair. The effect of delocalization in the calculated ν(N–H) and ν_{asym}(C–H) frequencies is underestimated, and it is overestimated in ν_{sym}(C–H), being always more pronounced in the MP2 frequencies. According to this agreement between observed and calculated frequencies, it can be confirmed that both N–H axial and equatorial envelope forms contribute to the vibrational spectrum. Furthermore, the T1 conformer should be also considered, because, as occurred with the electron diffraction and microwave data, the MP2 frequencies for E1 and T1 are compatible with the experimental values since the infrared spectra of both forms practically overlap in the regions where the N–H and C–H frequencies appear.

Conclusions

Hartree–Fock and Møller–Plesset calculations indicate that the preferred conformational process for the interconversion between the N–H axial and equatorial forms of PYR is pseudorotation and not the inversion of the ring through the planar form. The energy barrier for this process is approximately 0.6 kcal mol^{-1}, whereas the planar form is clearly less stable (>5 kcal mol^{-1}) than the envelope and twist forms. The variation of the puckering amplitude *q* indicates an elliptical pseudorotation path connecting the different forms which are interchanged during the process.

The description of the pseudorotational potential is heavily dependent on the computational model used. At the HF level,

non-polarized basis sets are not recommended, since they predict results considerably different from those obtained using higher basis sets. Beyond 6-31G**, the increase in the size of the basis set provides similar results, although for the group of basis sets used in this study (up to 6-311++G**), the convergence in the energy difference between the stable conformers has not yet been reached. When electronic correlation is introduced, the results obtained are significantly different from the HF ones. The second-order perturbative treatment, MP2, seems to be sufficient for considering the effect of electron correlation, since MP3 and MP4 produce similar results. These levels with the 6-31G** basis set predict that the equatorial form E6 is ~0.2 kcal mol^{-1} less stable than a group of isoenergetic forms which coexist around the form E1, in an interval situated approximately between $\varphi = 324°$ and $\varphi = 36°$, where the pseudorotation is free.

According to the NBO analysis of the HF/6-31G** wavefunctions, the energy difference between the N–H axial and equatorial forms is a consequence of the balance between the hyperconjugative and steric contributions. The equatorial form is stabilized because the delocalization of the nitrogen lone pair on the *trans* oriented C–H bonds (n_N–σ^*_{C-H}) is stronger than on the C–C bonds (n_N–σ^*_{C-C}). On the other hand, the steric interaction between the substituent on the nitrogen and the opposing C–H bonds destabilize the equatorial form. The delocalization of the lone pair determines the degree of puckering of these conformers and is the factor responsible for the different values taken by certain geometric parameters.

The comparison between the experimental data from microwave spectroscopy, electron diffraction and vibration frequencies, and the MP2/6-31G** theoretical results, indicates an acceptable quantitative agreement, hence this computational model could be considered to be the minimum necessary for obtaining an adequate description of the conformational preferences in PYR. On the other hand, the interpretation of the MP2 results in terms of the existence of a region of free pseudorotation in the vicinity of 0°, seems to eliminate the scattering in the interpretation of the different experimental results previously published.

One question remains open. At the MP2 level, the energy difference between the stable conformers is clearly dependent on the base, and even predicts different relative stabilities. Even for occasions where the MP2 corrections with certain basis sets could be considered artifacts, the influence of electron correlation on the description of PYR is clear, hence studies considering other models for correlation (CI, CC or DFT) should be carried out in the future.

Acknowledgements

The authors are indebted to the Xunta de Galicia for financial support and to the Centro de Supercomputación de Galicia (CESGA) for the use of computational facilities. I. P. J. wishes to thank the Spanish Ministerio de Educación y Ciencia for the award of an FPI grant.

References

1 J. Laane, Pseudorotation of Five-Membered Rings, in *Vibrational Spectra and Structure*, ed. J. R. Durig, Marcel Dekker, New York, 1972, vol. 1.
2 A. C. Legon, *Chem. Rev.*, 1980, **80**, 231.
3 H. L. Strauss, *Ann. Rev. Phys. Chem.*, 1983, **34**, 310.
4 W. J. Adams, H. J. Geise and L. S. Bartell, *J. Am. Chem. Soc.*, 1970, **92**, 5013.
5 H. J. Geise, W. J. Adams and L. S. Bartell, *Tetrahedron*, 1969, **25**, 3045.
6 G. G. Engerholm, A. C. Luntz, W. D. Gwinn and D. O. Harris, *J. Chem. Phys.*, 1969, **50**, 2446.
7 B. Cadioli, E. Gallinella, C. Coulombeau, H. Jobic and G. Berthier, *J. Phys. Chem.*, 1993, **97**, 7844.
8 D. Cremer and J. A. Pople, *J. Am. Chem. Soc.*, 1975, **97**, 1358.
9 J. A. Dobado, J. Molina Molina and M. Rodríguez Espinosa, *J. Mol. Struct.* (*THEOCHEM*), 1994, **303**, 205.
10 S. J. Han and Y. K. Kang, *J. Mol. Struct.* (*THEOCHEM*), 1996, **362**, 243.
11 J. E. Kilpatrick, K. S. Pitzer and R. Spitzer, *J. Am. Chem. Soc.*, 1947, **69**, 2483.
12 D. Cremer and J. A. Pople, *J. Am. Chem. Soc.*, 1975, **97**, 1354.
13 D. Cremer, *Isr. J. Chem.*, 1980, **20**, 12.
14 D. Cremer, *J. Phys. Chem.*, 1990, **94**, 5502.
15 D. L. Hildenbrand, G. C. Sinke, R. A. McDonald, W. R. Kramer and D. R. Stull, *J. Chem. Phys.*, 1959, **31**, 650.
16 J. C. Evans and J. C. Wahr, *J. Chem. Phys.*, 1959, **31**, 655.
17 J. P. McCullough, D. R. Douslin, W. N. Hubbard, S. S. Todd, J. F. Messerly, I. A. Hossenlopp, F. R. Frow, J. P. Dawson and G. Waddington, *J. Am. Chem. Soc.*, 1959, **81**, 5884.
18 K. S. Pitzer and W. E. Donath, *J. Am. Chem. Soc.*, 1959, **81**, 3213.
19 R. W. Baldock and A. R. Katritzky, *J. Chem. Soc. B*, 1968, 1470.
20 P. J. Krueger and J. Jan, *Can. J. Chem.*, 1970, **48**, 3236.
21 J. B. Lambert and W. L. Oliver, Jr., *J. Am. Chem. Soc.*, 1969, **91**, 7774.
22 J. B. Lambert, J. J. Papay, E. S. Magyar and M. K. Neuberg, *J. Am. Chem. Soc.*, 1973, **95**, 4458.
23 E. Breuer and D. Melumad, *J. Org. Chem.*, 1973, **38**, 1601.
24 J. B. Lambert, J. J. Papay, S. A. Khan, K. A. Kappauf and E. S. Magyar, *J. Am. Chem. Soc.*, 1974, **96**, 6112.
25 R. O. Duthaler, K. L. Williamson, D. D. Giannini, W. H. Bearden and J. D. Roberts, *J. Am. Chem. Soc.*, 1977, **99**, 8406.
26 W. Caminati, H. Oberhammer, G. Pfafferott, R. R. Filgueira and C. H. Gomez, *J. Mol. Spectrosc.*, 1984, **106**, 217.
27 G. Pfafferott, H. Oberhammer, J. E. Boggs and W. Caminati, *J. Am. Chem. Soc.*, 1985, **107**, 2305.
28 S. J. Han and Y. K. Kang, *J. Mol. Struct.* (*THEOCHEM*). 1996, **369**, 157.
29 L. Carballeira and I. Pérez-Juste, *J. Org. Chem.*, 1997, **62**, 6144.
30 L. Carballeira and I. Pérez-Juste, *J. Comput. Chem.*, in the press.
31 P. Pulay, *Mol. Phys.*, 1969, **17**, 197.
32 P. Pulay, *Mol. Phys.*, 1970, **18**, 473.
33 H. B. Schlegel, *J. Chem. Phys.*, 1982, **77**, 3676.
34 J. A. Pople, R. Krishnan, H. B. Schlegel and J. S. Binkley, *Int. J. Quantum Chem., Symp.*, 1979, **13**, 225.
35 C. Møller and M. S. Plesset, *Phys. Rev.*, 1934, **46**, 618.
36 J. A. Pople, R. Seeger and R. Krishnan, *Int. J. Quantum Chem., Symp.*, 1977, **11**, 149.
37 R. Krishnan and J. A. Pople, *Int. J. Quantum Chem.*, 1978, **14**, 91.
38 R. Krishnan, M. J. Frisch and J. A. Pople, *J. Chem. Phys.*, 1980, **72**, 4244.
39 T. K. Brunck and F. Weinhold, *J. Am. Chem. Soc.*, 1978, **102**, 1700.
40 J. P. Foster and F. Weinhold, *J. Am. Chem. Soc.*, 1980, **102**, 7211.
41 A. E. Reed and F. Weinhold, *J. Chem. Phys.*, 1985, **83**, 1736.
42 A. E. Reed, R. B. Weinstock and F. Weinhold, *J. Chem. Phys.*, 1985, **83**, 735.
43 A. E. Reed, L. A. Curtiss and F. Weinhold, *Chem. Rev.*, 1988, **88**, 899.
44 U. Salzner and P. v. R. Schleyer, *J. Org. Chem.*, 1994, **59**, 2138.
45 U. Salzner, *J. Org. Chem.*, 1995, **60**, 986.
46 *Gaussian 94* (*Revision B.2*), M. J. Frisch, G. W. Trucks, H. B. Schlegel, P. M. W. Gill, B. G. Johnson, M. A. Robb, J. R. Cheeseman, T. A. Keith, G. A. Petersson, J. A. Montgomery, K. Raghavachari, M. A. Al-Laham, V. G. Zakrzewski, J. V. Ortiz, J. B. Foresman, J. Cioslowski, B. B. Stefanov, A. Nanayakkara, M. Challacombe, C. Y. Peng, P. Y. Ayala, W. Chen, M. W. Wong, J. L. Andres, E. S. Replogle, R. Gomperts, R. L. Martin, D. J. Fox, J. S. Binkley, D. J. Defrees, J. Baker, J. P. Stewart, M. Head-Gordon, C. Gonzalez and J. A. Pople, Gaussian, Inc., Pittsburgh, PA, 1995.
47 For the sake of brevity, only the MP2/6-31G** optimized geometries are displayed in Table 2. The detailed geometries of the stationary points at the HF/3-21G and HF/6-31G** levels can be requested from the authors.
48 B. J. Teppen, M. Cao, R. F. Frey, C. Van Alsenoy, D. M. Miller and L. Schäfer, *J. Mol. Struct.* (*THEOCHEM*), 1994, **314**, 169.
49 E. Magnusson, *J. Am. Chem. Soc.*, 1993, **115**, 1051.
50 K. B. Wiberg, C. M. Hadad, T. J. LePage, C. M. Breneman and M. J. Frisch, *J. Phys. Chem.*, 1992, **96**, 671.
51 L. Schäfer, C. Van Alsenoy, J. O. Williams, J. N. Scarsdale and H. J. Geise, *J. Mol. Struct.* (*THEOCHEM*), 1981, **76**, 349.
52 P. J. Krueger and J. Jan, *J. Chem.*, 1970, **48**, 3229.
53 F. Bohlmann, *Chem. Ber.*, 1958, **91**, 2157.

Paper 8/01249K
Received 12*th February* 1998
Accepted 13*th March* 1998